



City Research Online

City, University of London Institutional Repository

Citation: Tsavdaridis, K. D., D'Mello, C. & Huo, B. Y. (2009). Shear Capacity of Perforated Concrete-Steel Ultra Shallow Floor Beams (USFB). Paper presented at the 6th National Concrete Conference, TEE, ETEK, 21-10-2009 - 23-10-2009, Paphos, Cyprus.

This is the unspecified version of the paper.

This version of the publication may differ from the final published version.

Permanent repository link: <https://openaccess.city.ac.uk/id/eprint/1046/>

Link to published version:

Copyright: City Research Online aims to make research outputs of City, University of London available to a wider audience. Copyright and Moral Rights remain with the author(s) and/or copyright holders. URLs from City Research Online may be freely distributed and linked to.

Reuse: Copies of full items can be used for personal research or study, educational, or not-for-profit purposes without prior permission or charge. Provided that the authors, title and full bibliographic details are credited, a hyperlink and/or URL is given for the original metadata page and the content is not changed in any way.

City Research Online:

<http://openaccess.city.ac.uk/>

publications@city.ac.uk

Computational Study Modelling the Experimental Work Conducted on the Shear Capacity of Perforated Concrete-Steel Ultra Shallow Floor Beams (USFB)

Konstantinos-Daniel TSAVDARIDIS¹, Cedric D'MELLO², Bing Yu HUO³

Key words: Ultra Shallow Floor Beam; Cellular Beams; Concrete Infill; Concrete Trapped; Bending Resistance; Finite Element Analysis of Concrete Beams

ABSTRACT : In modern building construction floor spans are becoming longer and one way of achieving this is to use composite beams. In order to minimize the structural depth of the composite sections, and to produce lighter members for economy reasons, steel perforated beams are designed to act compositely with the floor slab in an Ultra Shallow Floor Beam (USFB). In the USFB the concrete slab lies within the steel flanges and is connected through the web opening, providing enhanced longitudinal and vertical shear resistance. There is an additional benefit in increased fire resistance. The aim of this project is to investigate, through finite element simulations and suitable tests, the contribution of concrete in composite cellular beams in resisting vertical shear when the concrete slab lies between the flanges of the steel section. The concrete between the flanges provides the load path to transfer the shear force. For the computational approach to the problem, a three-dimensional Finite Element (FE) model was created, in which contact elements were implemented at the interface of the concrete and steel. In an earlier experimental study, four specimens of composite beams of similar concrete strength were tested under monotonic loading in order to produce reliable results. One specimen was from a lower grade of concrete and was tested in order to calibrate the shear resistance and the failure mode. One bare steel perforated section with web openings was also tested as a comparison. The comparison between the experimental and the computational results leads to useful conclusions. The results for the composite beams show a significant increase in shear resistance. The shear enhancement demonstrated in this study can now be used in design practice.

^{1,3} PhD Candidate, School of Engineering and Mathematical Sciences, City University London, email: konstantinos.tsavdaridis.1@city.ac.uk, bing.huo.1@city.ac.uk

² Senior Lecturer, School of Engineering and Mathematical Sciences, City University London, email: C.A.D'Mello@city.ac.uk

INTRODUCTION

This research study concerns composite (steel-concrete) structures and in particular, composite beams. For standard composite construction, with the slab connected on top of the flange of the beam (**Figure 1**), research has shown that the concrete slab contributes significantly to the vertical shear strength. Tests on short-span composite plate girders with web openings were initially carried out by Narayanan et al. (1989) and Roberts and Al-Amery (1991). These tests showed that the shear strength of a composite plate girder is significantly higher than that of a steel plate girder alone, if adequate shear connectors are provided in the composite girder. In addition, the composite action under predominantly shear loading depends on the tensile or pullout strength of the shear connectors. Analytical models including a contribution from the slab were proposed for determining the shear strength of composite plate girders. Experiments conducted by Clawson and Darwin (1982) and Donahey and Darwin (1988) indicated that the behaviour of composite beams with web openings is largely controlled by the shear-moment ratio at the opening. Darwin and Donahey (1988) proposed an equation to express the ultimate shear-moment relationship for composite beams with web openings.

In order to minimise the structural depth of the composite sections, steel perforated beams are designed to act compositely with floor slabs lying within the steel flanges (i.e. USFB) (**Figure 2**). This recently established method of construction was investigated by Tsavdaridis et al. (2009). The concrete between the flanges enhances the load-carrying capacity by providing a load path to transfer the shear force. Longitudinal shear tests on different configurations performed at City University London indicate that the USFB acts as a fully bonded beam. The analysis that has been performed and presented herein, together with the experimental programme carried out by Tsavdaridis (2010), is the first such work on USFBs, and has resulted in a better understanding of the failure mechanisms and the ultimate shear capacity.

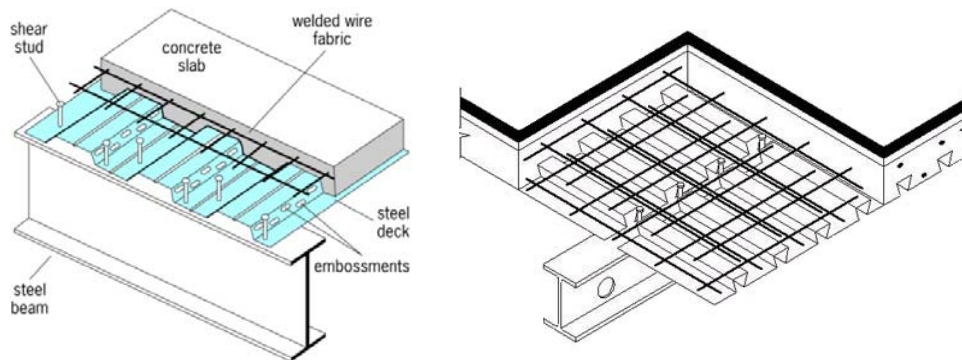


Figure 1. Typical composite construction adopted by McGraw-Hill Companies Inc. (left) and Corus (right).



Figure 2. USFB construction adopted by Westok Ltd.

OBJECTIVES AND SCOPE OF WORK

The objective of this work is to investigate, through FEM analysis, the enhanced vertical shear capacity of composite perforated beams when compared to bare perforated steel beams. In addition, the failure modes of the composite sections are investigated. As the results from this study are to be used in design practice, recommendations on the allowable nominal shear are to be made.

The scope of the present study is:

- To establish finite element models which are capable of predicting the structural behaviour of simply supported composite beams with large circular web openings where the concrete slab lies within the steel flanges.
- To examine both the ultimate load carrying capacities and the internal stress (crack) distributions of the composite beams, and to compare the results with those obtained from a previous experimental study.
- To perform a parametric study based on both concrete and steel material properties.

EXPERIMENTAL STUDY

A summary of the experimental work conducted on USFBs in the Engineering Laboratories at City University London is presented here. Further details of the tests are reported in Tsavdaridis et al. (2009).

A four-point bending load arrangement, with simply supported ends, was used, resulting in a pure bending moment distribution over the mid-span of the beams. The load was applied through two hydraulic jacks and a spreader plate. The applied load was obtained directly from load cells. The test arrangement is shown in **Figure 3**. To measure vertical deflection, three displacement transducers were

placed under the tension steel flange. Strain gauges were used only for the bare steel beams and were recorded for monitoring purposes and for comparison with the FE model.

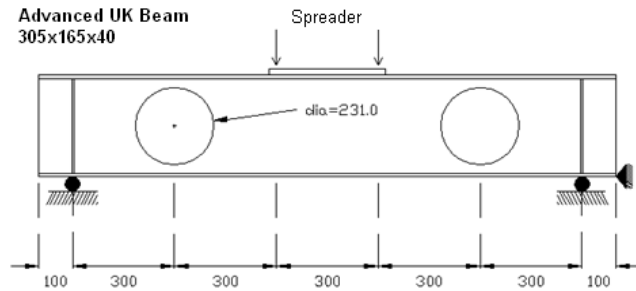


Figure 3. Test specimen configuration.

The steel section adopted for all tests was the UB305x165x40 of steel grade S275, with a web opening diameter, d_o , equal to 0.76 times the beam section depth. The distance between the openings and the support centre-line is equal to $1.3d_o$ and the beam is symmetrical about the mid-span centre-line. Five tests were conducted - three composite beams with similar concrete strengths at 14 days of curing, one with similar strength but after 52 days of curing (lower grade concrete) and a bare steel perforated beam. The specimens did not contain any reinforcement. A steel yield stress, f_y , of 318.25 MPa was taken from an average of several tensile coupon tests. The compressive concrete cubes' strength of all specimens are shown in "Table 1" together with the failure loads from the tests.

Table 1. Test results.

Specimen	USFB No.1	USFB No.2	USFB No.3	USFB No.4	Bare Steel
14-Day Compressive Strength of Concrete, f_{cu} (MPa)	27.9	26.8	25.3	25.6 (@ 52-Day)	N.A.
Ultimate Load Carrying Capacity f_{ult} (kN)	605	613	595	594	274

COMPUTATIONAL FE STUDY

Introduction

The analysis of general composite beams in flexure suggests that there is a close agreement between the test results and those from numerical simulations. For deeper beams working in flexure and shear where the contact surface is wider, there is a larger difference between predictions and test results, indicating that the problem is more complex. The use of FEM analysis to investigate the complex failure modes of USFBs is therefore appropriate as the problem is very complex. The model can be also used for further parametric studies. The ANSYS v11.0 FE programme was used in the analysis.

FE Model

A three-dimensional model was created with a fine mesh consisting of 68,569 elements. Regarding crack modelling in concrete, several researchers have studied the effect of element size in the nonlinear analysis of reinforced concrete structures (Shayanfar et al., 1997; Choi & Kwak, 1990), and they have shown that the results are indeed dependent on the finite element mesh size. Symmetry was used in the modelling; however, in the case of symmetry at mid-span, the way that the supports are modelled greatly affects the behaviour of the model, and in particular the position of the concrete cracks. Modelling of boundary conditions is often the most critical aspect in achieving sensible, reliable data from a finite element model (Baglin & Scott, 2000). As long as the load and the supports are applied on the steel beam and not on the concrete, the force can be applied directly on specific areas representing the loading plate and the roller supports. In order to avoid stress concentration problems and highly distorted elements, the load was applied as a pressure on an area and the supports modelled as restrictions of the degrees of freedom on areas.

It should be noted that in the analysis, no local buckling was allowed in the steel sections of the composite beams and hence the steel section is either plastic or compact. The structural configuration (i.e. two web openings well apart of each other) avoids failure of the beam by web-post buckling. This was confirmed by the experimental study.

Element and Material Models

Concrete: SOLID65 elements were used to model the concrete in ANSYS. The element is capable of plastic deformation and cracking in three orthogonal directions. These elements predict the non-linear behaviour of concrete materials using a smeared approach (William & Warnke, 1975) which has been adopted widely in recent years. It allows the elastic-plastic response of the reinforcement to be included in simulation. As no reinforcement is provided in the actual experiment, default values were kept for smeared reinforcement. Cracking and crushing are determined by a failure surface. The tensile strength is typically 8-15% of the compressive strength (Kachlakev, 2002). The ultimate concrete

compressive and tensile strengths for each beam model were calculated using similar constitutive formulas published by various researchers. Herein, the concrete in compression was modelled as an elastic-plastic material both with and without strain softening in order to have a better comparison with the experimental work (“Table 2”).

Steel: Typical SOLID45 elements were used to model the steel perforated beam with circular web openings. Steel was modelled as an elastic-plastic material with strain hardening and a bi-linear stress-strain relationship for both compression and tension. The Young’s Modulus and the Poisson’s Ratio of steel are taken as 205GPa and 0.3 respectively, while the values of yield and ultimate strengths used in the analysis were found after calibration against the experimental results and are shown in “Table 2”. An ultimate strain of around 0.25 was assumed for mild structural steel (Liang et al., 2005).

Shear Transfer Coefficient, $\beta_{1,2}$: Also called shear retention factor, it varies between ‘0’; for no aggregate interlock and ‘1’ for full aggregate interlock. Various shear transfer coefficients were used in this study for both open and closed cracks. High values were entered for the closed crack (e.g. 0.9, 1.0) so as to prevent possible fictitious crushing of the concrete before proper load transfer could occur through a closed crack.

Friction Coefficient, μ : No slip between concrete and steel was observed in the actual tests even after final failure was reached. Hence, a value of 1.0 (i.e. perfect bonding between steel perforated section and concrete) should be used for friction coefficient between the steel and concrete surface modelled in ANSYS. However, values from 0.0 to 0.9 were used in order to compare the results. The results showed an increase of stiffness in the strain results of the compressive top flange for beam with higher bond, but in the tensile flange the stiffness are almost identical. The reason for this could be the cracking of concrete in tensile zone which starts very early during the loading period.

Solution Method: The full Newton Raphson procedure was mainly used, even though this required the stiffness of the structure to be recalculated for each iteration. This procedure proved to be generally economical because much larger incremental steps were found to be possible. The automatic load control scheme was also employed.

Discussion and Comparison of Results

Good correlation between the test and numerical solutions depends on the assignment of accurate linear and non-linear material properties for both materials. (Liang et al., 2005; Parvanova et al., 2004; Kaewunruen & Remennikov, 2006). The parametric study was performed and a number of numerical solutions were analysed in order to evaluate the sensitivity of the various parameters. Various concrete compressive strength values were used in order to investigate the shear capacity enhancement of the composite beams. In

addition, the concrete tensile strength was varied taking into consideration the mesh size of concrete finite element and value of fracture energy, G_f . Also, various values of concrete Poisson's ratio, ν , were examined, as they are related to the condition (i.e. quality) of concrete. In order to simulate the experimental composite beam accurately, a steel yield stress with a reduction of 10.5 to 16.8% compared to average web-flange yield stress values, was used in most of the FE analyses performed. It can be seen that the ultimate capacity of the composite beams is governed by the steel strength.

The ultimate loads obtained from the parametric study were summarised in "Table 2" and presented in categories according to concrete compressive strength. The concrete cylinder strength $f_c=21.12MPa$ was also examined as it is the average value of the cube compressive concrete strength from four different USFB specimens, as they have reported by Tsavdaridis et. al (2009). The loads reported were the last applied load steps before the solution diverges due to the numerous cracks and large deflections. As a comparison, the ultimate load of the experimental beams was around 600kN.

Load Vs Deflection Relationships

Deflections are measured at mid-span at the centre of the bottom face of the beams. The results are satisfactorily correlated with the experiments where it is found that up to the ultimate load level no significant steel deflection occurred. Thereafter, the yielding of the steel explains the large concrete strains following the formation of large cracks, while a considerable drop in the load capacity is observed. It should be mentioned that at the lower the concrete compressive strength, the more cracks developed, although the capacity of the USFB did not change significantly. In the experiments large steel deflections ensue once the post-elastic curvature has occurred. The last descending branch of the load-deflection curve corresponds to a 'failure mechanism'. In the experimental work, failure was accompanied by wide intensive diagonal concrete crushing with the concrete pulling away from the steel section. This part of the load-deflection curve was not modelled as it needs significant computation effort and it is beyond the scope of this research study. Comparison of the load-deflection curves of some FE models presented in "Table 2" against the experimental test USFB No.1 are shown in **Figure 4**.

The finite element load-deflection curves and their stiffness correlate closely with the experimental curves. Observing the load-deflection behaviour of USFB it is noticed that when the first bending cracks were developed the curve become suddenly flat. However, while monitoring the experiment a smooth curve is observed. According to Parvanova et al. (2004) the ANSYS cracking model option does not fully include tensile stress relaxation, as the fracture energy parameter, G_f , is not included in the model as an important material constant.

Table 2. Material Parametric study of USFBs.

Steel		Cont.	Concrete					Results	Run
f_y (MPa)	$f_{ult.}$ (MPa) or $E_{Tan.}$	μ	f_c (MPa)	f_t (MPa)	ν	$\beta_{1,2}$	Refer. Theory Based	Failure Load (kN)	Code No.
ULTRA SHALLOW FLOOR BEAM									
265*	410	1.0	26.70	1.86	0.20	0.3,1.0	†	617	59
265*	410	1.0	26.70	1.86	0.17	0.3,1.0	†	627	3
265*	410	0.8	26.70	1.86	0.17	0.3,1.0	†	611	7
265*	410	0.3	26.70	1.86	0.17	0.3,1.0	†	548	8
265*	410	1.0	26.70	1.86	0.15	0.3,1.0	†	547	58
265*	410	1.0	26.70	1.86	0.15	0.6,0.6	†	555	16
265*	410	1.0	26.70	1.86	0.15	0.1,0.9	†	607	18
275**	$E_{Tan.}=200$	0.8	26.70	1.86	0.15	0.1,0.9	†	618	25
265*	410	1.0	26.70	1.86	0.15	1.0,1.0	†	635	19
265*	410	1.0	26.70	1.86	0.00	1.0,1.0	†	648	20
355*	530	1.0	26.70	1.86	0.20	0.3,1.0	†	617	11
355*	530	1.0	26.70	1.86	0.17	0.3,1.0	†	590	12
355*	530	0.0	26.70	1.86	0.17	0.3,1.0	†	470	13
265*	410	1.0	32.00	3.083	0.15	0.3,1.0	§	629	31
265*	410	0.8	32.00	3.083	0.15	0.3,1.0	§	615	32
265*	410	0.5	32.00	3.083	0.15	0.3,1.0	§	565	33
265*	410	0.9	32.00	3.524	0.2	0.3,1.0	¥	588	C1
275*	410	0.9	32.00	3.524	0.2	0.3,1.0	¥	611	C4
285*	350	0.9	32.00	3.524	0.2	0.3,1.0	¥	641	C5
285**	$E_{Tan.}=20$	0.9	32.00	3.524	0.2	0.3,1.0	¥	622	C6
355*	499	0.9	32.00	3.524	0.2	0.3,1.0	¥	742	B1
275*	410	0.9	20.00	2.786	0.2	0.3,1.0	¥	577	B5
275*	410	0.6	20.00	2.786	0.2	0.3,1.0	¥	563	B6
355*	499	0.9	20.00	2.786	0.2	0.3,1.0	¥	730	B2
355**	$E_{Tan.}=20$	0.9	20.00	2.786	0.2	0.3,1.0	¥	734	B3
355*	530	0.9	20.00	2.786	0.2	0.3,1.0	¥	733	B4
275*	410	0.9	21.12	1.839	0.3	0.3,1.0	#	545	B9
275*	410	0.9	21.12	2.863	0.2	0.3,1.0	¥	584	B10
275*	410	0.4	21.12	2.863	0.2	0.3,1.0	¥	508	C8
275*	410	1.0	21.12	2.863	0.2	0.3,1.0	¥	591	B11
STEEL PERFORATED									
318.25*	430	---	---	---	---	---	---	352	75
265*	410	---	---	---	---	---	---	331	60
355**	$E_{Tan.}=2000$	---	---	---	---	---	---	352	61

*MISO – Multi-linear Isotropic Hardening Plasticity is adopted

**BISO – Bi-linear Isotropic Hardening Plasticity is adopted

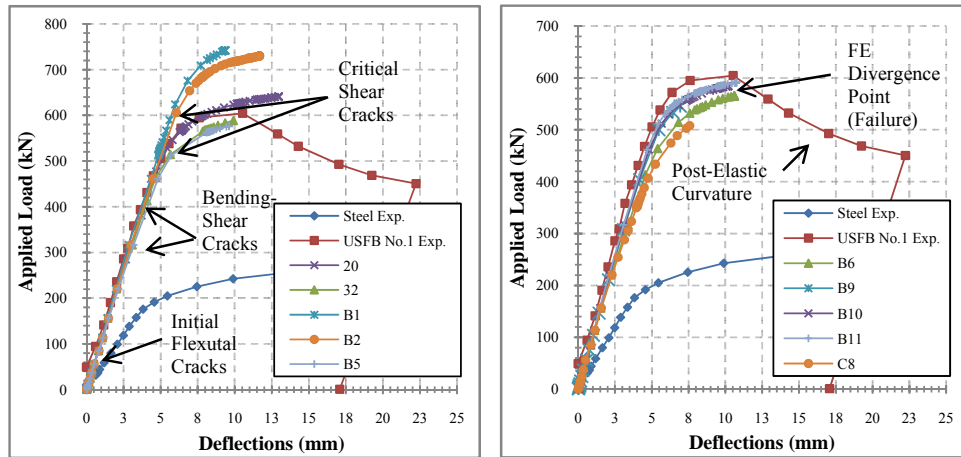


Figure 4. Force-deflection curves comparison between experimental test (USFB No.1) and various numerical solutions from “Table 2”.

Crack Patterns for Concrete – Failure Mode

As it is aforementioned many numerical tests were performed simulating this particular composite beam using different constitutive options and parameters. It can be seen that the flexural and the diagonal (flexural-shear) cracks affect the failure mode and the ultimate load carrying capacity. In **Figure 5** the crack development is shown at four different load steps in order to show the crack propagation.

Nonlinear numerical solutions were capable of replicating the full range cracks including the pure flexural, flexural shear and the critical shear crack. Smeared cracks are spread over the high shear stress region and occur mostly at the ends of the beam between the support and loading area (**Figure 6**). The path of shear cracks follows the trajectory of the principal stresses and can also be seen in the experimental study. The finite element program accurately predicts that the composite beams fail in shear and also numerous cracks occur at mid-span rather than underneath the loading location.

Analytically, diagonal shear failure begins with the development of few vertical flexural cracks at the mid-span, followed by a destruction of the bond between the bottom steel flange and the concrete. A critical shear diagonal crack develops in the vicinity of the web opening of the steel perforated beam.

Finally, the slip between steel and concrete, when using a value other than 1 for the friction coefficient, is obtained together with the contact surface condition for a typical USFB subjected to flexural loading and are presented in **Figure 7**.

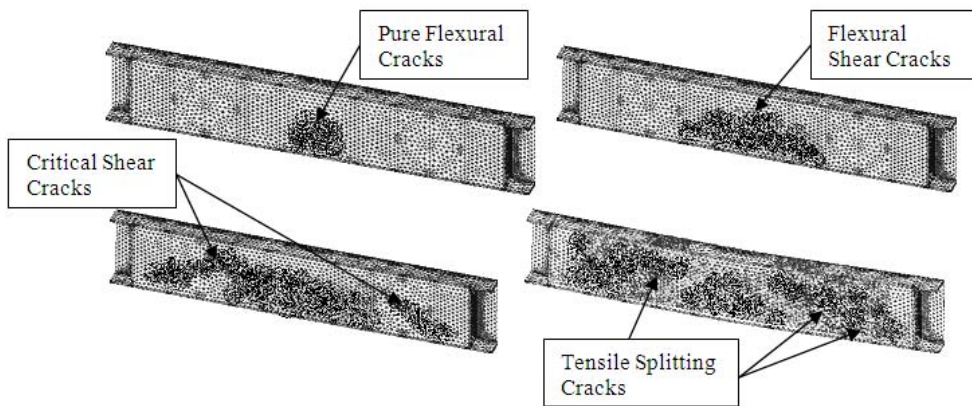


Figure 5. Bending and shear crack development at the front side of the beam.

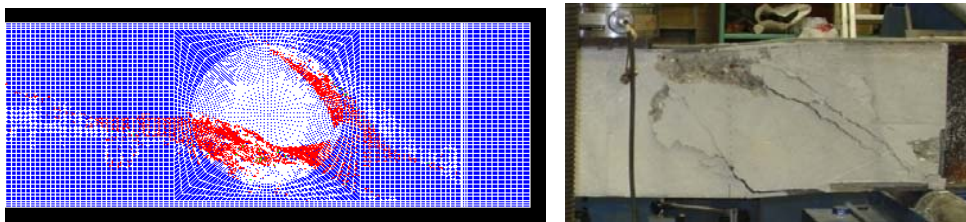


Figure 6. Comparison of crack patterns of USFB No. 2 (right) at failure point adopted by Tsavdaridis et al. (2009).

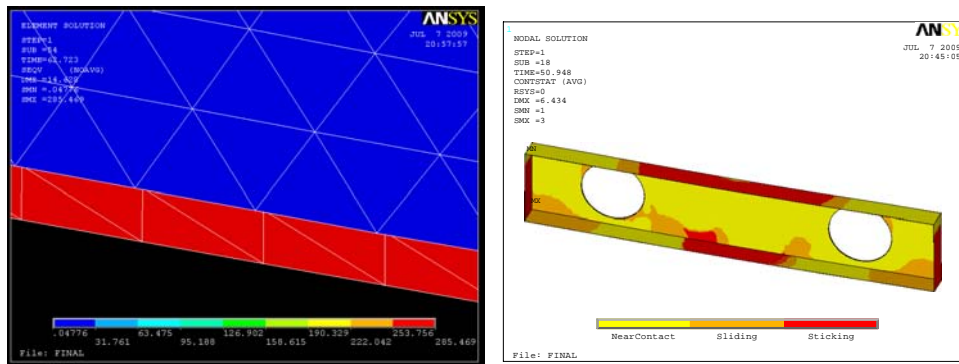


Figure 7. Sliding between steel and concrete (left) and contact surface condition (right) of the USFB.

CONCLUSIONS

The results of the ANSYS FE analyses generally show very well agreement with observations and data from the experimental full-scale beam tests conducted previously by the authors at City University London. The parametric study conducted, and the variation of parameters illustrates how the Ultra Shallow Floor Beam behaves. These FE models can now be used in further studies to develop design rules for USFBs.

Based on the analytical study presented in this paper, the following conclusions can be drawn:

- Due to the concrete infill the ultimate vertical load carrying capacity of the USFBs doubled when compared to the corresponding bare steel beam.
- The results agree with the experiments in that in composite beams the concrete fails first before any significant distortion of steel web occurs.
- All cracks in the FE analysis seem to develop at a higher load compare to that observed in the experiments. This was probably due to micro-cracks in the experimental specimens.
- Whilst the concrete compressive strength affects the strength of the USFBs, the ultimate load carrying capacity is dominated by the steel strength.
- Numerous researchers have published different constitutive formulas that model the concrete material properties. A sensitivity study of these constitutive relations found that they affect the load carrying capacity of USFBs differently.
- The values of these material parameters and some “correction” factors were obtained to accurately simulate the experimental tests for USFBs.
- The shear resistance of USFB section with perforated steel section with large web openings and without reinforcement consists of contributions from the concrete in compression and aggregate interlock.
- USFBs behave as fully bonded composite elements and this correlated well with experiments.

REFERENCES

- ANSYS (2009), User’s Manual Revision 11, ANSYS, Inc., Canonsburg, PA
- BS EN 197: Part 1: 2000. Cements. Composition, specifications and conformity criteria for common cements, BSI, UK, (2000)
- Clawson, W.C. & Darwin, D., “Tests of composite beams with web openings”. J. Struct. Div. ASCE, Vol. 1, No 108 (1982) 145-162

- Darwin, D. & Donahey, R.C., "LRFD for composite beams with unreinforced web openings". J. Struct. Div. ASCE, Vol. 3, No 114 (1988) 535-552
- Donahey, R.C. & Darwin, D., "Web openings in composite beams with ribbed slabs". J. Struct. Div. ASCE, Vol. 3, No 114 (1988) 518-534
- Hirst, M.J.S. & Yeo, M.F., "The analysis of composite beams using standard finite element programs". Comput. Struct., Vol. 3, No 11 (1980) 223-237
- Narayanan, R., Al-Amery, R.I.M. & Roberts, T.M., "Shear strength of composite plate girders with rectangular web cut-outs". J. Constr. Steel Res., Vol. 2, No 12 (1989) 151-166
- ¥ Kachlakev D. & Miller T., "FE Modeling of Reinforced Concrete Structures Strengthened with FRP Laminates", Oregon State University, Department of Transportation, Final Report SPR 316 (2001)
- # Kaewunruen, S. & Remennikov, A., "Nonlinear finite element modelling of railway prestressed concrete sleeper", in Proceedings of the 10th East Asia-Pacific Conference on Structural Engineering and Construction (Bangkok Thailand August 3-5, 2006), Bangkok, Thailand (2006) 323-328
- § Liang, Q.Q., Uy, B., Bradford, M.A. & Ronagh, H.R., "Strength analysis of steel-concrete composite beams in combined bending and shear", J. Struct. Eng., Vol. 131, No 10 (2005) 1593-1600
- † Parvanova, S.P., Kazakov, K.S., Kerelezova, I.G., Gospodinov, G.K. & Nielsen, M.P., "Modelling the nonlinear behaviour of R/C beams with moderate shear span and without stirrups using ANSYS", Faculty of Civil Eng., Sofia, Research for the National Science Fund under the contract № TH-1406/04, Technical Report (2004)
- Roberts, T.M. & Al-Amery, R.I.M., "Shear strength of composite plate girders with web cutouts". J. Struct. Eng., Vol. 7, No 117 (1991) 1897-1910
- Tsavdaridis, K. D. "Failure modes of composite and non-composite perforated steel beams sections with various shapes and sizes of web openings", PhD thesis in preparation (supervised by Dr. C. D'Mello), School of Engineering and Mathematical Sciences, City University, London, (2010)
- Tsavdaridis, K.D., D'Mello, C. & Hawes, M., "Experimental study of ultra shallow floor beams with perforated steel sections", 11th Nordic Steel Construction Conference (Malmö Sweden September 2-4, 2009) NSCC2009 Press, Malmö, Sweden (2009)
- Wang, A.J. & Chung, K.F., "Advanced finite element modelling of perforated composite beams with flexural shear connectors". J. Struct. Eng., Vol. 30, No 10 (2008) 2724-2738
- William, K.J., & Warnke, E.P., "Constitutive model for triaxial behaviour of concrete", in Proceedings of International Association of Bridge and Structural Engineering Conference (Bergamo Italy, 1974) ISMES Press, Bergamo, Italy (1974) Vol.19., 174